

Cavity QED with quantum dots in semiconductor microcavities

M. T. Rakher*, S. Strauf, Y. Choi, N.G. Stolz, K.J. Hennessey, H. Kim, A. Badolato, L.A. Coldren,
E.L. Hu, P.M. Petroff, D. Bouwmeester
University of California Santa Barbara, Santa Barbara, CA, USA 93106;

ABSTRACT

Cavity quantum electrodynamic (QED) effects are studied in semiconductor microcavities embedded with InGaAs quantum dots. Evidence of weak coupling in the form of lifetime enhancement (the Purcell effect) and inhibition is found in both oxide-apertured micropillars and photonic crystals. In addition, high-efficiency, low-threshold lasing is observed in the photonic crystal cavities where only 2-4 quantum dots exist within the cavity mode volume and are not in general spectrally resonant. The transition to lasing in these soft turn-on devices is explored in a series of nanocavities by observing the change in photon statistics of the cavity mode with increasing pump power near the threshold.

Keywords: quantum dot, photonic crystal, micropillar, microcavity, low threshold laser, cavity QED, photon statistics

1. INTRODUCTION

Many proposed implementations of quantum communication and computation in condensed matter systems rely on having a strong interaction between a localized two-level system and a high quality cavity mode [1, 2]. If the coupling strength (which is inversely proportional to the square root of the mode volume) between the two oscillators is weak compared to the lifetime of either the emitter or the cavity mode, then the coupling is said to be in the weak coupling regime. In this regime, the primary effect of the cavity mode is to enhance the lifetime of the emitter and this is called the Purcell effect [3]. This Purcell enhancement factor is proportional to the ratio of the quality factor (Q) of the cavity mode to the effective mode volume (V_{eff}). In addition, if the emitters can provide enough gain to compensate for the cavity decay rate, then lasing may be observed. In the case of semiconductor microcavities embedded with quantum dots (QDs), both of these interesting phenomena can be studied.

2. DEVICE GROWTH AND FABRICATION

2.1 InGaAs Quantum Dots embedded in Oxide-Apertured Micropillar Cavities

A low-density, single layer of InGaAs, self-assembled quantum dots is grown by molecular beam epitaxy in the Stranski-Krastanow growth mode. InGaAs islands are partially covered with GaAs and then annealed before completely capping with GaAs. This process shifts the emission spectrum of the QDs to the blue (near 930 nm) where Silicon-based single photon counting detectors work more efficiently. A low density of these QDs acts as the active region between two high quality AlGaAs/GaAs distributed Bragg reflector (DBR) mirrors. Just above the QD active region an oxide aperture is introduced [4]. This aperture is created by oxidizing a thin layer of pure AlAs, forming Al_xO_y . This oxidation is allowed to proceed until a small aperture of roughly $2\ \mu\text{m}$ is created in the center. The Al_xO_y has a lower index of refraction than the surrounding material so the aperture acts as a lens and confines the mode to the center of the pillar. This has a two-fold effect; it keeps the field away from the sidewalls, which limits the Q of most micropillars, and it reduces the mode volume. In total, it serves to increase the Purcell factor. The pillars are defined by optical lithography and reactive ion etch and a SEM image of one is shown in Fig 1. An array of devices is created with varying total pillar diameter to achieve the optimum Purcell factor and account for small errors in oxidation time.

*rakher@physics.ucsb.edu

2.2 InGaAs QDs embedded in Photonic Crystal Membrane Cavities

Using a similar low density QD sample, photonic crystal (PC) cavities are formed by defining a triangular lattice of air holes by electron beam lithography. Then, holes are created along with the membrane by chemical etching in HF. Line defect cavities are formed by selective removal of 3, 7 or 11 holes (L3, L7, and L11 cavities) to create a defect region. An example of a SEM image of an L3 cavity is shown in Fig. 1. Strong optical confinement in the plane is provided by the 2-D photonic crystal while out of plane confinement is provided by the GaAs air interface at the top and bottom of the membrane. Device parameters such as hole radius, lattice spacing, and membrane thickness are optimized to provide the highest Q while keeping the mode volume as small as possible.

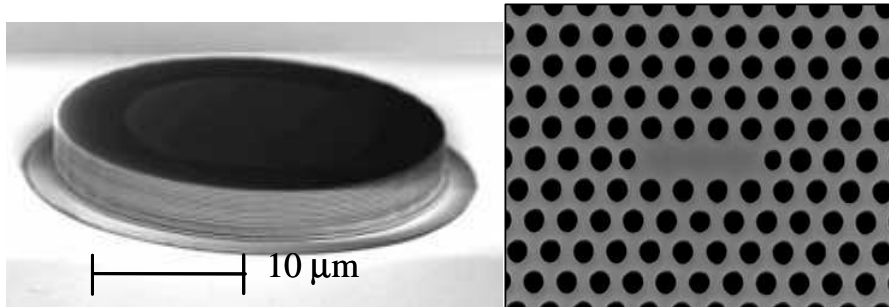


Fig. 1. Scanning electron microscope (SEM) images of an oxide-apertured micropillar (left) and an L3 PC cavity (right).

3. EXPERIMENTAL SETUP

3.1 QD and Device Spectroscopy

The QDs and the devices are primarily studied using micro-photoluminescence spectroscopy. The samples are kept in a He-flow cryostat operated at 4.2 K with a heater capable of increasing the temperature to 300 K. Carriers are excited in the samples by a pulsed 82 MHz Ti:Sa laser with approximately 100 fs pulse width. This laser is primarily operated at 850 nm to excite carriers resonantly into the wetting layer. Additionally, continuous wave lasers operating at 780 nm and 632.8 nm can be used for above-bandgap excitation. These sources are focused through a 50X objective with NA = 0.55 onto the sample surface as shown in Fig. 2. Emission is imaged through the same objective where it is picked off by a beamsplitter (BS) and directed into a 1.25 m spectrometer with a liquid nitrogen cooled CCD array, yielding a 30 μ eV spectral resolution at 900 nm.

3.2 Lifetime and Hanbury-Brown and Twiss Measurements

Lifetime measurements of single QDs are performed with pulsed excitation using a single photon counting avalanche photodiode in conjunction with a time-to-amplitude converter card. Before detection, single QD spectral lines are chosen and spectrally filtered with a 0.5 nm bandpass filter as shown in Fig. 2. Hanbury-Brown and Twiss measurements are performed by incorporating a beamsplitter and another single photon detector as shown in Fig 2. This measures the second-order coherence of the emitted light and can be used to determine information about the photon statistics of the emitted light field.

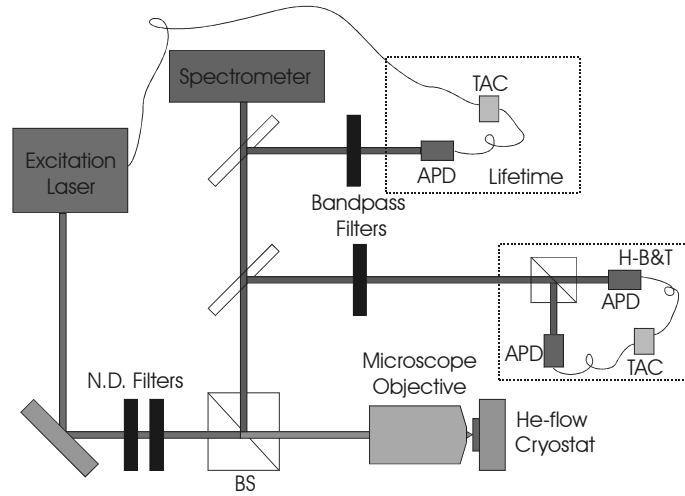


Fig. 2. A schematic of the experimental setup. The excitation laser is directed through an objective onto the sample surface. The collected photoluminescence can then be directed into the spectrometer, the lifetime setup, or the Hanbury-Brown and Twiss setup.

4. RESULTS

4.1 Cavity mode spectra

As shown in Fig. 3, the fabrication processes described in the previous section display high Q cavity modes in the spectral region of QD s-shell transitions. The spectra from the micropillar (Fig. 3) can be analyzed to determine the Q and values greater than 30000 (the resolution limit of the spectrometer) have been measured [5]. Comparing the mode spacing to values predicted from simulations, the mode volume can be determined to be approximately $51 (\lambda/n)^3$. This yields an expected Purcell factor of around 72. The photonic crystal spectra can be analyzed to determine the Q and values nominally around 12000 are obtained. Mode volume calculations have been carried out by finite-difference time-domain simulations and typical values for the lowest order mode are around $0.68 (\lambda/n)^3$.

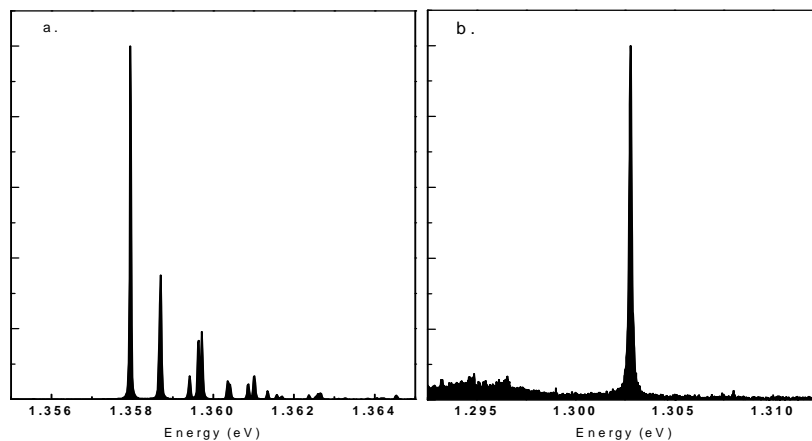


Fig. 3. Micro-photoluminescence spectra of cavity modes in the micropillar structure (a.) and the L3 photonic crystal cavity (b.). Both measurements were done at 4.2 K with the pump power high enough to saturate the QD transitions.

4.2 QD lifetime measurements

Measurements of single QD lifetimes on and off resonance with the cavity mode have also been carried out. Lifetimes for dots on resonance with micropillar cavity modes have been shown to be as small as 200 ps (our measurement resolution), corresponding to a Purcell factor of more than 6. As shown in Fig 4a, the lifetime decreases as the dot is brought into resonance with the cavity mode as expected by the Purcell effect. Measurements of QDs in photonic crystal cavities have shown lifetimes as long as 10 ns as shown in Fig 4b. This suggests that while the QD may be in spectral resonance with the cavity mode, its lifetime is inhibited due to spatial displacement from the cavity field maximum. Enhanced lifetimes are much harder to obtain experimentally due to the small probability of a dot being both spatially and spectrally on resonance with the cavity mode.

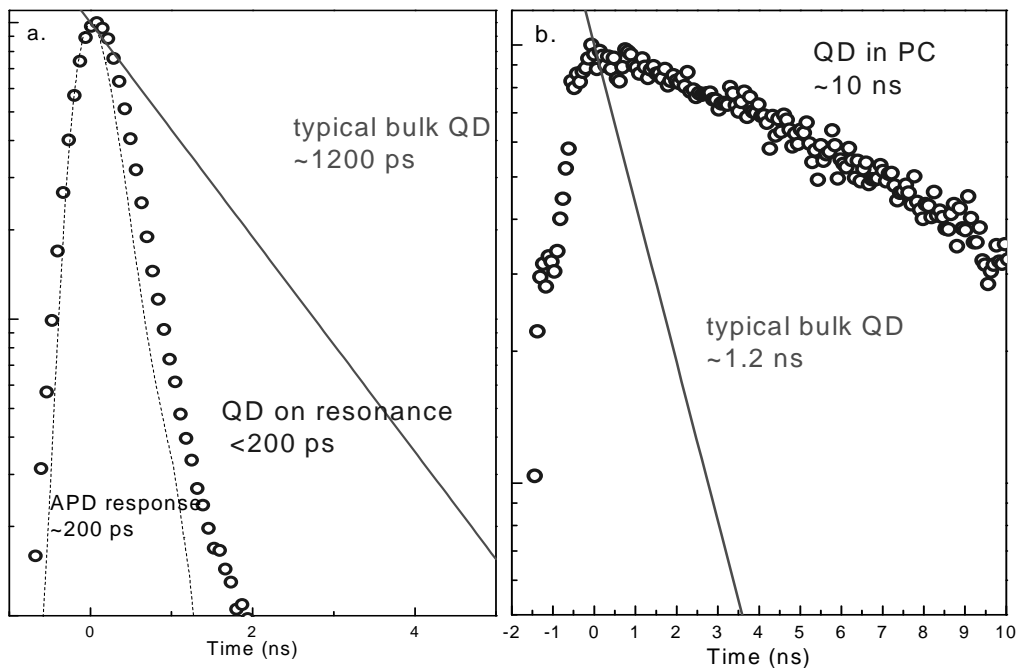


Fig. 4. a). A plot of the lifetime of a single QD on resonance with a micropillar cavity mode. The lifetime measurement is limited by the APD response (shown as the segmented line) of 200 ps. For comparison, a line showing a typical bulk QD lifetime of 1200 ps is shown. b). A plot of a QD inside a photonic crystal structure demonstrating a lifetime around 10 ns. This strong inhibition of the lifetime suggests the dot is spatially displaced from the maximum of the field. A typical bulk QD lifetime is shown for comparison.

4.3 Lasing in PC cavities

Analysis of the intensity and linewidth of PC cavity modes as a function of input pump power reveals lasing behavior in these devices as shown in Figure 5. The soft-turn on and low-threshold characteristics of these cavities demonstrates a high coupling of spontaneous emission into the mode, called the β factor, of around 0.85 [6]. Lasing was unexpected due to the extraordinarily low QD density as well as the fact that the sharp transition lines of the QDs are not spectrally resonant with cavity mode. Because of the high β factor, the onset of lasing action is hard to distinguish from other sources of nonlinear output behavior.

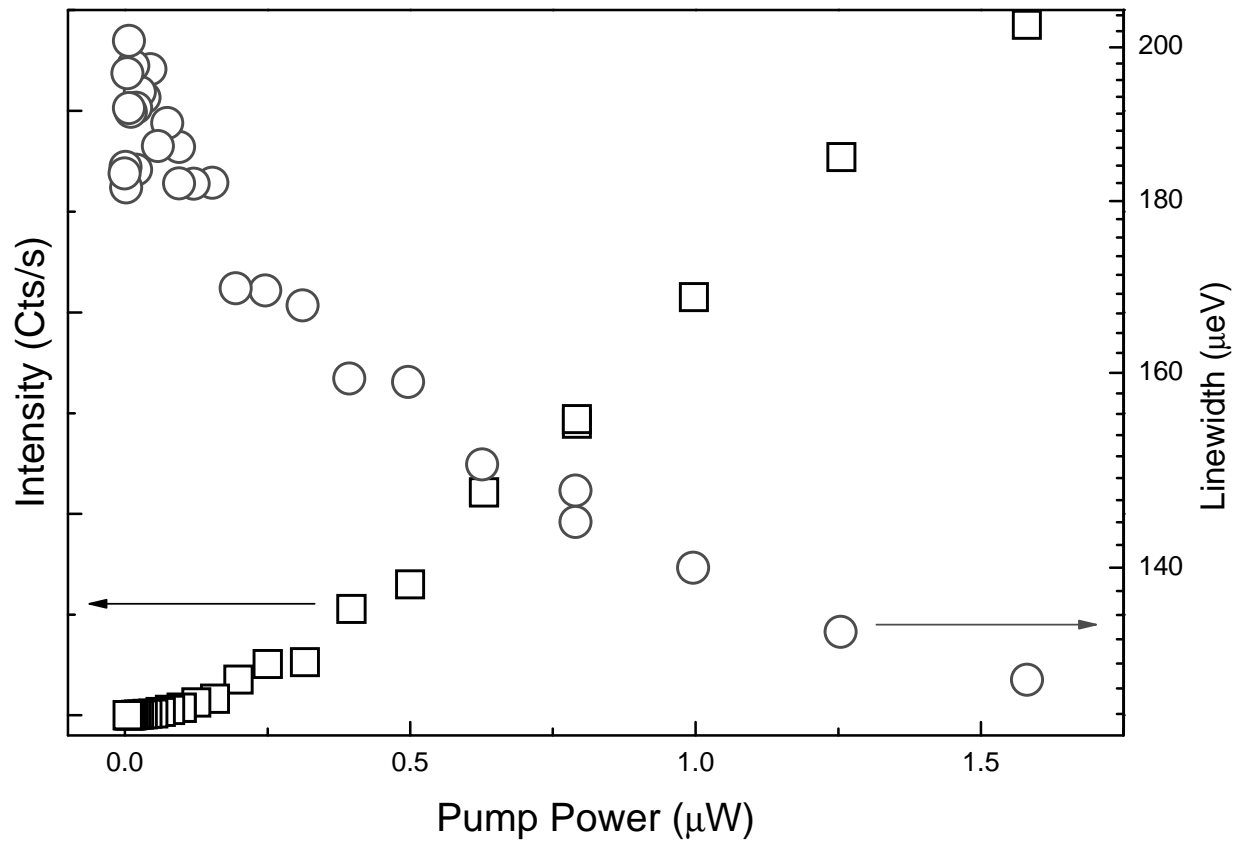


Fig. 5. Output count rate and linewidth of an L3 cavity mode vs. input power from a continuous wave 780 nm source.

4.4 Second-order correlation measurements for PC lasers

To validate the onset of lasing in the PC cavity devices, second order intensity correlation measurements were performed at pump powers near the lasing threshold. As shown in Figure 6, $g^{(2)}(0)$ increases to a value near 2 and then subsequently diminishes to 1 as the pump power is increased. Theoretically, one expects the photon statistics of a cavity mode below the laser threshold to behave like a thermal light source, corresponding to $g^{(2)}(0) = 2$. Once lasing is established, the photon statistics are described by a coherent state with Poissonian statistics, corresponding to $g^{(2)}(0) = 1$. The results in Figure 6 demonstrate exactly that aside from the initial increase. This initial increase is attributed to the transition from the uncorrelated spontaneous emission regime to the stimulated emission regime. If the mode is comprised of uncorrelated spontaneous emission events, $g^{(2)}(0) = 1$. Once stimulated emission sets in, $g^{(2)}(0)$ tends toward the thermal value of 2.

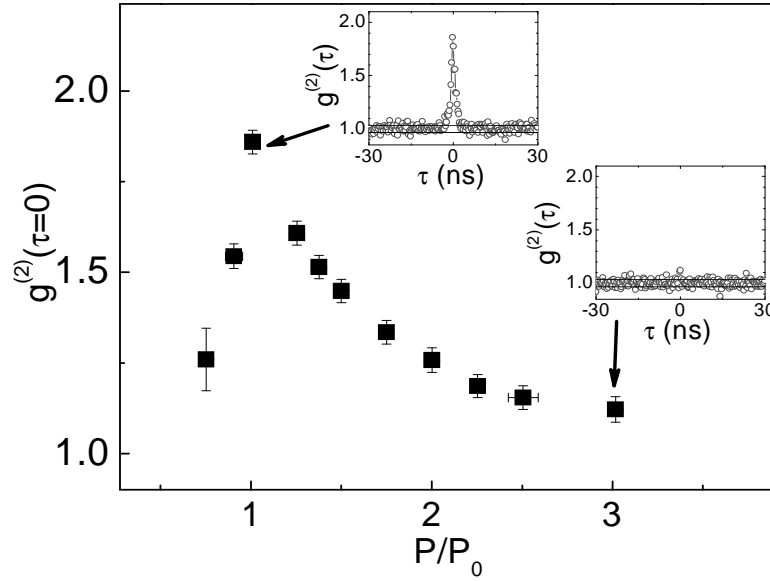


Fig. 6. $g^{(2)}(0)$ vs. threshold normalized pump power for an L11 laser. The insets show the corresponding $g^{(2)}(\tau)$ at two of the measured pump powers.

5. CONCLUSIONS

In conclusion, a wide variety of phenomena associated with cavity QED have been investigated using InGaAs quantum dots embedded in two different semiconductor nanocavity structures. Weak coupling in the form of the Purcell spontaneous emission enhancement has been experimentally found for QDs interacting with oxide-apertured micropillar cavity modes and strong inhibition has been demonstrated for QDs inside photonic crystal defect cavities. While a strong enhancement has not been found for PC cavities, advances in active QD positioning will enable future experiments in both the weak and strong coupling regimes [7].

Surprisingly, the photonic crystal cavities demonstrated the onset of lasing with increasing pump power. This was unexpected considering the low QD density along with the spectral mismatch of the sharp s-shell transitions and the cavity mode. Subsequent measurements of the photon statistics as a function of pump power near the lasing threshold validate the claim of lasing and are an important addition to the standard input-output and linewidth measurements. They are an essential measurement because of the soft turn-on nature of these high β , low threshold lasers, which can make identification of lasing action difficult [6].

REFERENCES

1. A. Imamoglu, et. al, "Quantum Information Processing Using Quantum Dot Spins and Cavity QED," *Phys. Rev. Lett.* **83**, 4204 (1999).
2. P. Michler, et. al, "A Quantum Dot Single-Photon Turnstile Device," *Science* **290** 2282 (2000).
3. K. J. Vahala, "Optical Microcavities," *Nature* **424**, 839 (2003).
4. N.G. Stolz, et. al, "Quantum Dot Spontaneous Emission Lifetime Modification in Optical Microcavities using Oxide Apertured Micropillars," *Proc. SPIE* **6101**, 61010W (2006).
5. N.G. Stolz, et. al, "High quality factor optical microcavities using oxide apertured micropillars," *App. Phys. Lett.* **87**, 031105 (2005).
6. S. Strauf, et. al, "Self-tuned quantum dot gain in photonic crystal lasers," *Phys. Rev. Lett.* **96**, 127404 (2006).
7. A. Badolato, et. al, "Deterministic Coupling of single quantum dots to single nanocavity modes," *Science* **308**, 1158 (2005).